

## HADRON RADIATION IN $\tau$ PRODUCTION AND THE LEPTONIC $Z$ BOSON DECAY RATE<sup>†</sup>

A.H. Hoang<sup>§</sup>, J.H. Kühn<sup>‡</sup> and T. Teubner<sup>§</sup>

Institut für Theoretische Teilchenphysik, Universität Karlsruhe,  
D-76128 Karlsruhe, Germany

### Abstract

Secondary radiation of hadrons from a tau pair produced in electron positron collisions may constitute an important obstacle for precision measurements of the production cross section and of branching ratios. The rate for real and virtual radiation is calculated and various distributions are presented. For  $Z$  decays a comprehensive analysis is performed which incorporates real and virtual radiation of leptons. The corresponding results are also given for primary electron and muon pairs. Compact analytical formulae are presented for entirely leptonic configurations. Measurements of  $Z$  partial decay rates which eliminate all hadron and lepton radiation are about 0.3% to 0.4% lower than totally inclusive measurements, a consequence of the  $\mathcal{O}(\alpha^2)$  negative virtual corrections which are enhanced by the third power of a large logarithm.

### 1. Introduction

Since the turn on of LEP several years ago experiments have collected an impressive amount of data, with a combined sample of more than  $10^7$  hadronic and  $10^6$  leptonic events. This enormous event rate has allowed us to measure the ratio of hadronic versus leptonic events or the leptonic decay rate with an accuracy of better than two per mill. Clearly, at this level of precision subtle aspects of radiative corrections have to be taken into account. One specific example is the  $Z$  decay rate into a lepton pair: Details of the treatment of additional radiation of a pair of soft leptons or of a soft hadronic system have a strong impact on the predicted rate. Formally the rate of these events is of order  $(\alpha/\pi)^2 \approx 5 \cdot 10^{-6}$ . In reality, however, these events are enhanced by the third power of a large logarithm, which essentially compensates one factor of  $\alpha/\pi$ . This positive contribution is to a large extent cancelled by the corresponding virtual correction, leaving a small positive shift in the inclusive rate. The dominant part of this shift can be incorporated into the corrections of order  $\alpha/\pi$  by employing the running QED coupling  $\alpha(Q^2)$ , the remainder is truly negligible. However, in an experimental analysis which eliminates events with secondary radiation the large negative virtual corrections must be taken into account.

---

\*The complete postscript file of this preprint, including figures, is available via anonymous ftp at [ttpux2.physik.uni-karlsruhe.de](ftp://ttpux2.physik.uni-karlsruhe.de) (129.13.102.139) as `/ttp95-17/ttp95-17.ps` or via www at <http://ttpux2.physik.uni-karlsruhe.de/cgi-bin/preprints/> Report-no: TTP95-17.

<sup>†</sup>Work supported by BMFT 056 KA 93P.

<sup>‡</sup>Present address: SLAC, Stanford University, Stanford, CA 94309.

<sup>§</sup>e-mails: [hoang@ttpux2.physik.uni-karlsruhe.de](mailto:hoang@ttpux2.physik.uni-karlsruhe.de) and [tt@ttpux2.physik.uni-karlsruhe.de](mailto:tt@ttpux2.physik.uni-karlsruhe.de)

With this motivation in mind we present in this paper a comprehensive study of virtual and real leptonic and hadronic radiation. Particular emphasis is put on the radiation of hadrons from a primary  $\tau$  lepton pair. This is the most difficult reaction to evaluate, since three independent scales  $s$ ,  $m_\tau$  and  $m_{had}$  enter the calculation. The results for the radiation of hadrons from an electron or muon pair are significantly simpler: The lepton mass is far smaller than the threshold for hadron production and can be safely set to zero throughout the calculation. Results for this latter case have been given in [1] for virtual corrections in the high energy approximation. The corresponding case for real final state radiation with a massless primary lepton has been solved in analytic form in [2, 3]. The virtual and real radiation of a lepton pair off a massive primary lepton has been evaluated for arbitrary  $s$  in [4] for the special case that the mass of the secondary lepton is far smaller than all other scales of the problem. In this paper we complete this topic by considering radiation of hadrons from a primary  $\tau$  pair. Since large data samples of  $\tau$  pairs are also collected at lower energies, e.g. at around 10 GeV, this case also is scrutinized. However, it is observed that radiation is far less important in this low energy region, an obvious consequence of the less prominent role of the “large” logarithms. Hadronic radiation off primary  $\tau$  pairs also plays a special role from a purely practical point of view:  $\tau$  leptons decay into hadrons (plus a neutrino) and hence events with additional hadron radiation might well be considered experimentally as hadronic final states, since they have larger hadronic multiplicity and the invariant mass of the hadronic subsystems exceeds  $m_\tau$ . By the same token, the measurement of  $\tau$  decays into large multiplicity final states could in principle be influenced by inappropriate assignment of the radiative events. Last but not least, signals of “new” physics could be faked by a misinterpretation of these Standard Model reactions.

The final state radiation discussed in this paper is complementary to the initial state radiation treated in [1, 5]. No interference terms are present between radiation from the initial and final state as long as the (dominant) QED reactions are considered and axial vector couplings from neutral current reactions are ignored. Final state radiation of lepton (and quark) pairs has also been treated in [6] in the context of a Monte Carlo Program. For hadron radiation this approach turns out to be inadequate, since the reaction is dominated by low mass hadronic systems. For lepton radiation our results are lower than those of [6] by about 15%. An important ingredient for the evaluation of real and virtual hadronic radiation is a proper description of  $R(s)$ , which has to be taken from experiment. In our approach we employ the most recent parametrization of data taken from [7].

The plan of this paper is as follows: In section 2 the “master formula” for calculation of the total rate is presented, which is at the same time a convenient starting point for a variety of differential distributions. The case of real radiation with primary  $\tau$ -leptons and secondary hadrons is discussed in some detail, considering high energies ( $\sqrt{s} = M_Z$ ) as well as  $\sqrt{s} = 10$  GeV (characteristic for a  $B$  factory) and 4.2 GeV (relevant for a  $\tau$ -charm factory). Predictions for the total rate are presented, as well as distributions which are differential with respect to the mass of the hadronic system and its energy. The corresponding virtual radiation is calculated in section 3 for the same c.m. energies and at the  $\tau$  pair threshold. Corrections are given for the Dirac and Pauli form factor, as well as for the total rate. Section 4 is concerned with a detailed discussion of  $Z$  decays. Results for electron, muon and tau as primary leptons are presented both for hadronic and leptonic radiation. The corresponding predictions for virtual radiation are also collected. It is demonstrated that these virtual corrections reduce the exclusive leptonic rate of the  $Z$  boson by several per mill. Section 5 contains a summary and our conclusions.

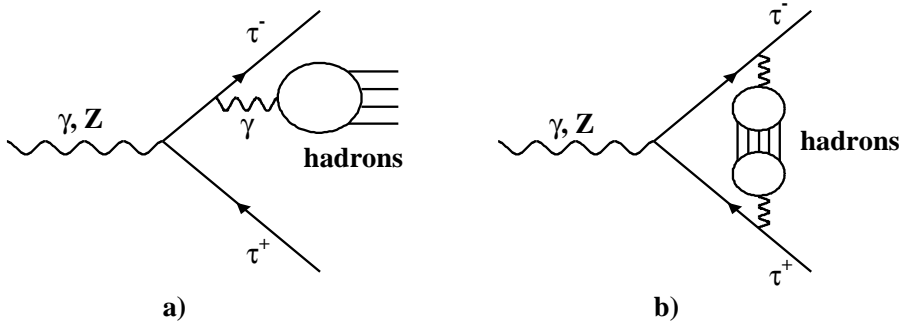


Figure 1: *Typical diagrams for real and virtual emission of hadrons in  $\tau$  pair production.*

## 2. Real radiation

The calculation of the ratio  $\sigma_{\tau^+\tau^-had}/\sigma_{pt}$  (where  $\sigma_{pt} = 4\pi\alpha^2/3s$ ) can be reduced to the numerical evaluation of the two dimensional integral

$$R_{\tau^+\tau^-had} \equiv \frac{\sigma_{\tau^+\tau^-had}}{\sigma_{pt}} = \frac{1}{3} \left(\frac{\alpha}{\pi}\right)^2 \int_{4m_\tau^2}^{(\sqrt{s}-2m_\tau)^2} \frac{ds'}{s'} R_{had}(s') F(s'/s), \quad (1)$$

$$F(z) = 4 \int_{4m_\tau^2/s}^{(1-\sqrt{z})^2} dy \left\{ -\sqrt{1 - \frac{4m_\tau^2}{sy}} \Lambda^{1/2}(1, y, z) \left[ \frac{1}{4} + \frac{\frac{2m_\tau^2}{s} + \frac{4m_\tau^4}{s^2} + \left(1 + \frac{2m_\tau^2}{s}\right)z}{(1-y+z)^2 - \left(1 - \frac{4m_\tau^2}{sy}\right) \Lambda(1, y, z)} \right] \right. \\ \left. + \frac{\frac{2m_\tau^4}{s^2} + \frac{m_\tau^2}{s}(1-y+z) - \frac{1}{4}(1-y+z)^2 - \frac{1}{2}(1+z)y}{1-y+z} \ln \frac{1-y+z - \sqrt{1 - \frac{4m_\tau^2}{sy}} \Lambda^{1/2}(1, y, z)}{1-y+z + \sqrt{1 - \frac{4m_\tau^2}{sy}} \Lambda^{1/2}(1, y, z)} \right\}$$

where

$$\Lambda(1, y, z) = 1 + y^2 + z^2 - 2(y + z + yz).$$

$F(s'/s)$  can be interpreted as the normalized cross section for  $\tau$  pair production with the additional emission of a vector boson of mass  $\sqrt{s'}$ . The integral in (1) sums up all hadronic contributions of mass  $\sqrt{s'}$  weighted by  $R_{had}(s')$ . The numerical treatment of this integral allows us to use experimental input for the function  $R_{had}(s')$  and avoids the poor approximations of a parton model inspired calculation. In contrast to [4] — there we solved the integrals analytically in the case where the “massive” photon splits into a pair of fermions with mass far smaller than  $m_\tau$  —  $F(s'/s)$  is calculated numerically. We would like to emphasize that (1) contains no restriction on the mass values and is thus also applicable to completely different kinematical situations. In the limit of vanishing external mass  $m_\tau = 0$  we recover eq. (2) of [2] for  $F(s'/s)$ .

The physical situation described by (1) consists typically of a  $\tau$  pair with large invariant mass and a hadronic state with low invariant mass (see also the discussion of our results below). The hadrons are emitted relatively collinear with one of the  $\tau$  leptons. The reverse configuration, where a  $\tau$  pair is radiated off the corresponding quark via a virtual photon could be treated with a similar technique. This final state would consist mainly of quite soft and collinear virtual photons leading to a  $\tau$  pair of low invariant mass and is therefore easily distinguished from the situation we focus on in this letter. As far as the total rate is concerned, the interference term between these two amplitudes vanishes if the production is induced by the (electromagnetic or neutral) vector current. For axial

vector induced contributions the interference term is different from zero. However, this term does not exhibit a mass singularity in the limit of vanishing quark or leptonic mass and thus is not enhanced by a large logarithm. It can be neglected in all cases of interest. In the limit of vanishing fermion mass this interference term has been calculated in [8].

For most of this paper we will discuss the total rate for secondary radiation. However, eq.(1) contains implicitly also information on single and double differential distributions. The integration variable  $s'$  denotes the squared hadronic mass. The square of the invariant mass of the primary  $\tau^+\tau^-$  system, on the other hand, is given by  $y \cdot s$ , which can be easily related to the energy  $E_{had}$  of the hadronic system. The single differential distribution  $dR_{\tau^+\tau^-had}/ds'$  is trivially obtained from eq.(1). The energy distribution of the radiated hadronic system is given by

$$\begin{aligned} \frac{dR_{\tau^+\tau^-had}}{dE_{had}} = & \\ & \frac{4}{3} \left(\frac{\alpha}{\pi}\right)^2 \int_{s'_{min}}^{E_{had}^2} \frac{ds'}{s s'} R_{had}(s') \left\{ -\sqrt{1 - \frac{4m_\tau^2}{s y}} \sqrt{E_{had}^2 - s'} \left[ 1 + \frac{2m_\tau^2 + \frac{4m_\tau^4}{s} + \left(1 + \frac{2m_\tau^2}{s}\right) s'}{E_{had}^2 - \left(1 - \frac{4m_\tau^2}{s y}\right) (E_{had}^2 - s')} \right] \right. \\ & \left. + \frac{s}{E_{had}} \left( \frac{2m_\tau^4}{s^2} + \frac{2E_{had}m_\tau^2}{s^{3/2}} - \frac{E_{had}^2}{s} - \frac{1}{2} \left(1 + \frac{s'}{s}\right) y \right) \ln \frac{E_{had} - \sqrt{1 - \frac{4m_\tau^2}{s y}} \sqrt{E_{had}^2 - s'}}{E_{had} + \sqrt{1 - \frac{4m_\tau^2}{s y}} \sqrt{E_{had}^2 - s'}} \right\} \quad (2) \end{aligned}$$

with

$$s y = s + s' - 2E_{had}\sqrt{s} \quad \text{and} \quad s'_{min} = \max\left(4m_\tau^2 - s + 2E_{had}\sqrt{s}, 4m_\pi^2\right). \quad (3)$$

These formulae will be useful below.

In the numerical evaluation of (1) we use experimental data for  $R_{had}(s')$  as presented in [7]<sup>1</sup>. A convenient approach adapted to the experimental procedure is to decompose the hadronic final states into continuum and resonance contributions. Following [7], the two pion contribution ( $\hat{=}\rho$ ) is taken into account together with the continuum by a direct integration of data points. The most important narrow resonances are added separately using the narrow width approximation<sup>2</sup>, which is accurate enough for our purposes. More details about  $R_{had}(s')$  are given in the appendix.

In Table 1 we display the continuum plus  $\rho$  and the resonance contributions separately for different center of mass energies  $\sqrt{s} \leq M_Z$ . The contribution from a virtual  $Z$  as intermediate state remains unimportant up to  $\sqrt{s} \approx M_Z$ . They are strongly suppressed for obvious kinematical reasons as can be easily seen in Table 1 (see also discussion below). This in turn justifies neglecting radiation through the virtual  $Z$ . In Fig. 2  $R_{\tau^+\tau^-had}$  is plotted for the range  $2m_\tau < \sqrt{s} < M_Z$ . The rise of  $R_{\tau^+\tau^-had}$  and  $R_{\tau^+\tau^-l+l^-}$  for increasing  $\sqrt{s}$  is easily understood from the leading term in the high energy limit proportional to the third power of the logarithm of  $s$ , i.e.  $\ln^2(m_{had}^2/s) \ln(m_\tau^2/s)$ ,  $m_{had}$  being a characteristic hadronic mass scale of  $\mathcal{O}(300 \text{ MeV})$ . (For leptonic radiation these logarithms can be calculated explicitly, see eq. (8).)

As an interesting exercise one may apply (1) to  $\tau^+\tau^-q\bar{q}$  production where the quarks are again radiated off the tau leptons leaving  $\tau$  pairs of large invariant mass<sup>3</sup>. This leads to a parton model like prediction of  $R_{\tau^+\tau^-had}$ . Adopting the quark mass values of [6], viz.  $m_u = m_d = m_s = 300 \text{ MeV}$ ,  $m_c = 1.5 \text{ GeV}$  and  $m_b = 4.5 \text{ GeV}$  and choosing  $\sqrt{s} = 10 \text{ GeV} / M_Z$  one would predict

<sup>1</sup>We thank F. Jegerlehner and S. Eidelman for providing their compilation of data and discussing its proper treatment.

<sup>2</sup>Masses and electronic widths are taken from [9].

<sup>3</sup>In this case one just has to use  $R(s') = N_c Q_q^2 \left(1 + \frac{2m_q^2}{s'}\right) \sqrt{1 - \frac{4m_q^2}{s'}}$  in the numerical integration.

$\sqrt{s}$	4.2 GeV	10 GeV	$M_Z$
$\sqrt{s'_{max}}$	0.646 GeV	6.446 GeV	87.63 GeV
Channel			
$2\pi$	$5.11 \cdot 10^{-9}$	$2.07 \cdot 10^{-5}$	$1.81 \cdot 10^{-4}$
$\omega$	–	$2.19 \cdot 10^{-6}$	$2.08 \cdot 10^{-5}$
$\phi$	–	$2.81 \cdot 10^{-6}$	$3.22 \cdot 10^{-5}$
$J/\psi$	–	$3.54 \cdot 10^{-7}$	$2.82 \cdot 10^{-5}$
$\Upsilon$	–	–	$8.17 \cdot 10^{-7}$
Continuum (with $R_{had}(s')$ from experiment):			
0.81 up to 4.98 GeV	–	$1.22 \cdot 10^{-5}$	$2.59 \cdot 10^{-4}$
4.98 up to 10 GeV	–	$7.13 \cdot 10^{-9}$	$0.60 \cdot 10^{-4}$
10 up to 25 GeV	–	–	$0.30 \cdot 10^{-4}$
25 up to 40 GeV	–	–	$0.03 \cdot 10^{-4}$
Continuum (with perturbative $R_{had}(s')$ )			
$\sqrt{s'} > 40$ GeV	–	–	$3.70 \cdot 10^{-7}$
$R_{\tau^+\tau^-had}$	$5.11 \cdot 10^{-9}$	$3.82 \cdot 10^{-5}$	$6.14 \cdot 10^{-4}$
$R_{\tau^+\tau^-e^+e^-}$	$2.75 \cdot 10^{-5}$	$4.05 \cdot 10^{-4}$	$1.82 \cdot 10^{-3}$
$R_{\tau^+\tau^-\mu^+\mu^-}$	$1.14 \cdot 10^{-7}$	$2.82 \cdot 10^{-5}$	$2.94 \cdot 10^{-4}$
$R_{\tau^+\tau^-\tau^+\tau^-}$	–	$3.07 \cdot 10^{-8}$	$3.13 \cdot 10^{-5}$
Sum	$2.76 \cdot 10^{-5}$	$4.71 \cdot 10^{-4}$	$2.76 \cdot 10^{-3}$

Table 1: Contributions to  $R_{\tau^+\tau^-had}$  and values of  $R_{\tau^+\tau^-l^+l^-}$  ( $l = e, \mu, \tau$ ) for center of mass energies  $\sqrt{s} = 4.2$  GeV/10 GeV/ $M_Z$ .  $\sqrt{s'_{max}}$  is the upper limit of the phase space integral (1).

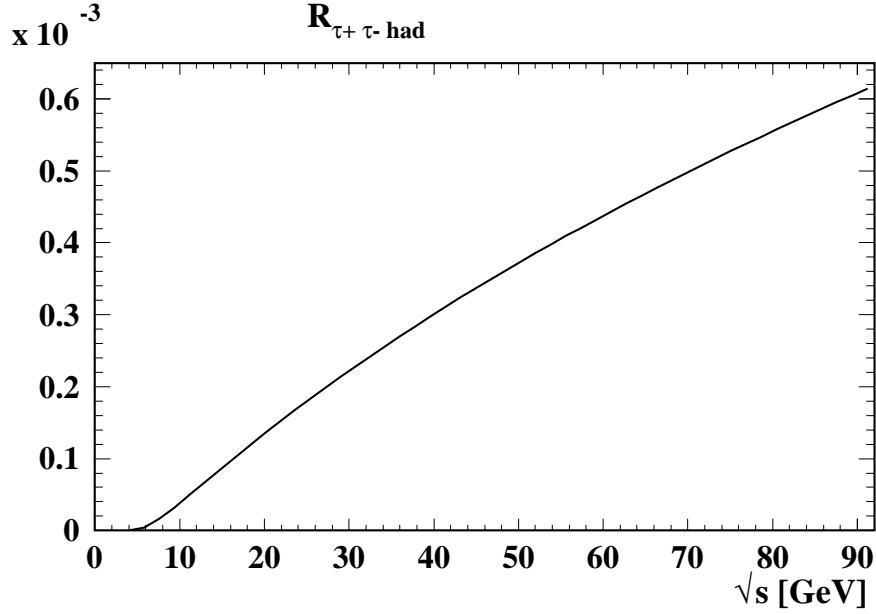


Figure 2: Normalized cross section  $R_{\tau^+\tau^-had}$ .

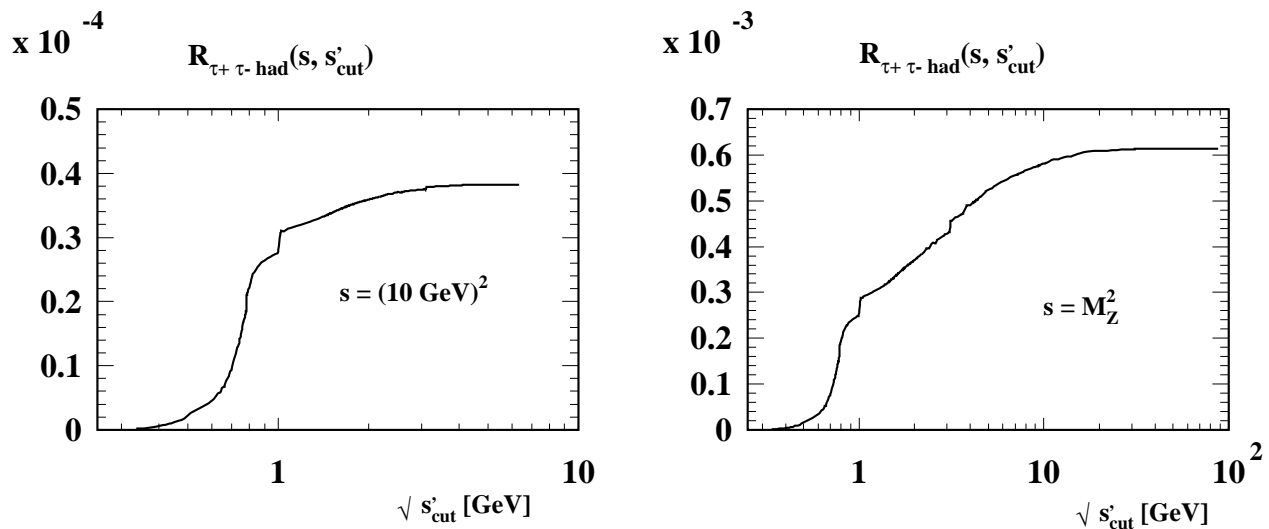


Figure 3: *Dependence of the normalized cross section  $R_{\tau^+\tau^-had}$  from a cut  $s'_{cut}$  for  $\sqrt{s} = 10$  GeV and  $\sqrt{s} = M_Z$ .*

$$\begin{aligned}
R_{\tau^+\tau^-u\bar{u}} &= 4 R_{\tau^+\tau^-d\bar{d}} = 4 R_{\tau^+\tau^-s\bar{s}} = 1.1 \cdot 10^{-5} / 2.1 \cdot 10^{-4}, \\
R_{\tau^+\tau^-c\bar{c}} &= 1.2 \cdot 10^{-7} / 5.1 \cdot 10^{-5}, \\
R_{\tau^+\tau^-b\bar{b}} &= 0 / 2.6 \cdot 10^{-6}, \\
R_{\tau^+\tau^-had} &= 1.7 \cdot 10^{-5} / 3.7 \cdot 10^{-4}.
\end{aligned} \tag{4}$$

It is obvious that this model underestimates the production rate by about a factor of two. (The same phenomenon has also been observed for hadron radiation off muons and electrons [2].) For energies near the  $\tau^+\tau^-$  production threshold a parton model like prediction is completely impossible without artificial tuning of the masses of the light quark flavours.

For completeness we also list in Table 1 the rate for the radiation of lepton ( $e, \mu, \tau$ ) pairs. The prediction for the radiation of  $e^+e^-$  and  $\mu^+\mu^-$  is based on the analytical formula given in [4], the one for  $\tau^+\tau^-\tau^+\tau^-$  is obtained through numerical integration. An adequate approximation (better than 1%) for  $R_{\tau^+\tau^-\tau^+\tau^-}$  at  $\sqrt{s} = M_Z$  is presented in eq. (9) at the end of section 4.

Table 1 and Fig. 2 demonstrate that hadronic radiation may become important for precision measurements of  $\tau$  branching ratios on top of the  $Z$ . Radiation of  $e^+e^-$  or  $\mu^+\mu^-$  may even be of relevance in the 10 GeV region, e.g. at a  $B$  meson factory.

It is evident that experimental sensitivity and the probability to assign  $\tau^+\tau^-$  events with hadronic radiation to exclusive or inclusive  $\tau$  pair production depends strongly on the invariant mass of the hadronic system. As mentioned above the integral (1) is in fact dominated by small  $s'$ . In the numerical approach this is easily shown by replacing the upper limit of the integral in (1) by a value  $s'_{cut} < s'_{max} = (\sqrt{s} - 2m_\tau)^2$ . In Fig. 3 we display our results for  $R_{\tau^+\tau^-had}(s, s'_{cut}) = \sigma_{\tau^+\tau^-had}(s, s'_{cut}) / \sigma_{pt}$  for  $\sqrt{s} = 10$  GeV/ $M_Z$ . Even for  $Z$  decays 86% of the integral originates from  $\sqrt{s'} < 5$  GeV and 58% from  $\sqrt{s'} < m_\tau$ . In Fig. 4 we present the differential distributions  $dR_{\tau^+\tau^-had}/ds'$  and  $dR_{\tau^+\tau^-had}/dE_{had}$  for  $\sqrt{s} = 10$  GeV /  $M_Z$  using eqs.(1) and (2). Contributions from the narrow resonances are not taken into account for the distributions  $dR_{\tau^+\tau^-had}/ds'$  but can easily be read off from Table 1. As expected the distributions are peaked at small  $s'$  (already evident from Fig. 3) and at fairly small  $E_{had}$  illustrating that hadronic radiation is clearly dominated by the  $\rho$ -resonance. It is not inconceivable that these events might affect precision measurements of multipion decay modes of the  $\tau$ . In view of possible

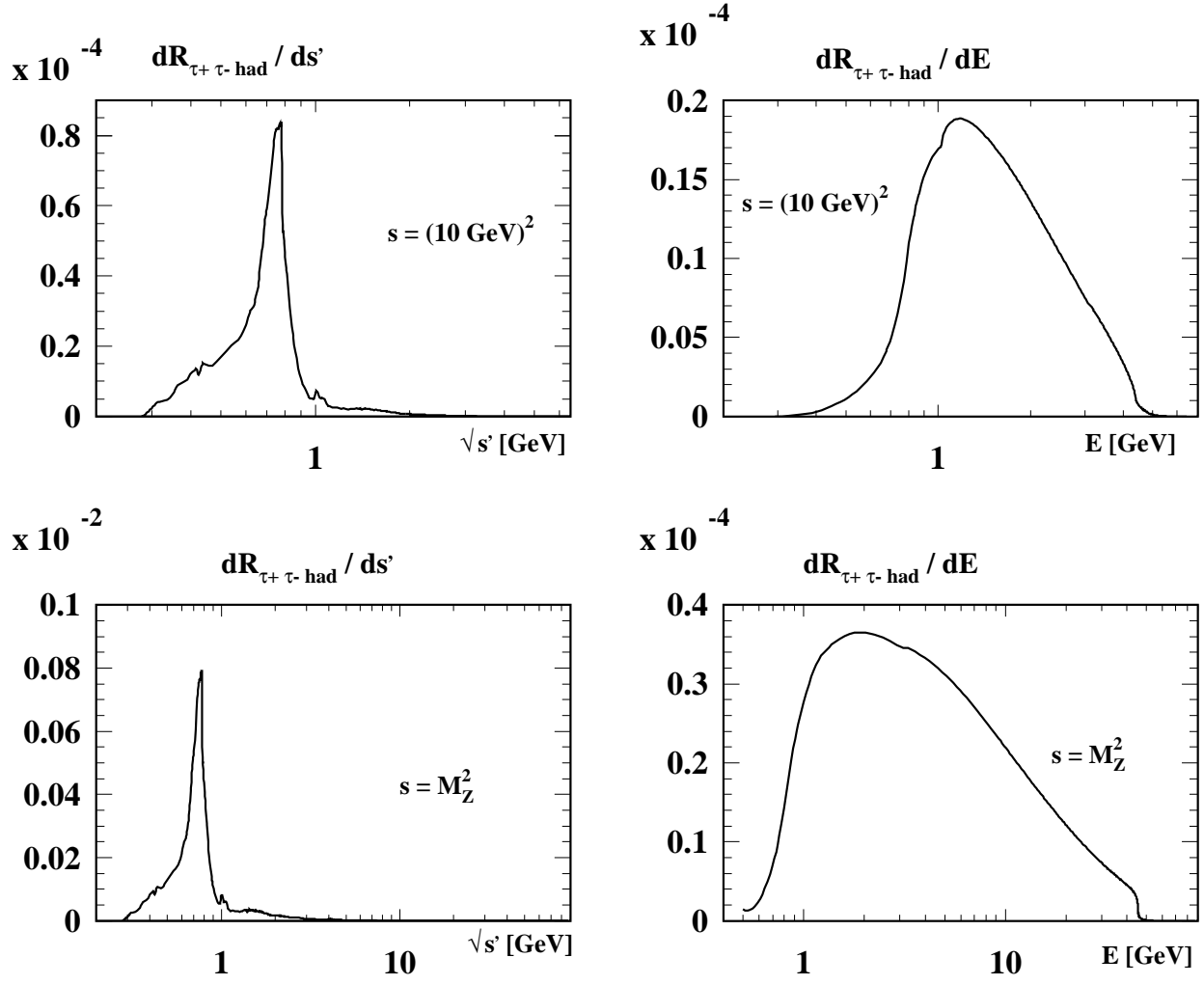


Figure 4: *Differential distributions for real emission of hadrons in  $\tau$  pair production as described in the text.*

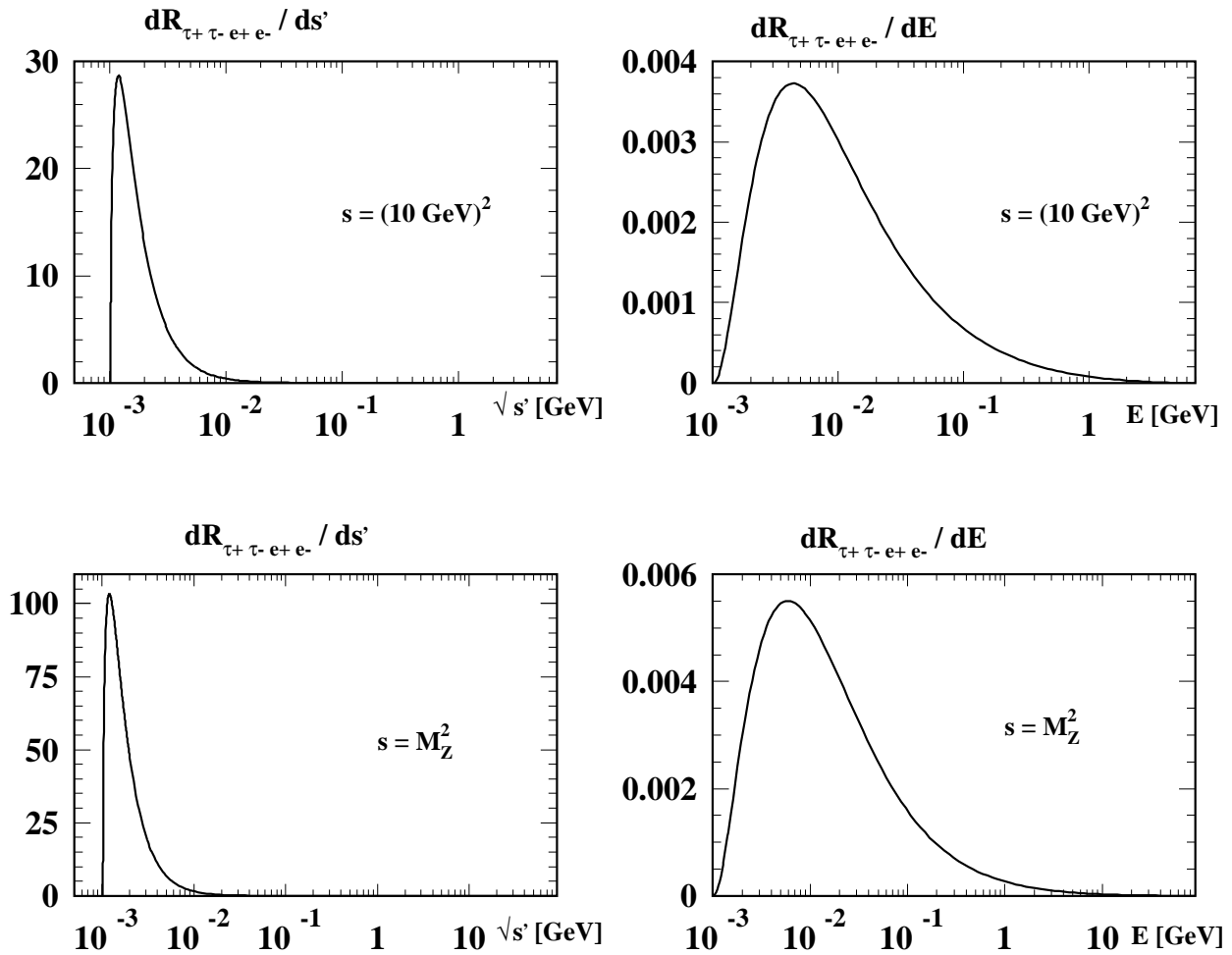


Figure 5: *Differential distributions for real emission of  $e^+e^-$  in  $\tau$  pair production as described in the text.*

experimental applications we also present in Fig. 5 the differential distributions  $dR_{\tau^+\tau^-e^+e^-}/ds'$  and  $dR_{\tau^+\tau^-e^+e^-}/dE_{e^+e^-}$  for the radiation of electron–positron pairs at  $\sqrt{s} = 10$  GeV and at  $M_Z$ . These are evidently also peaked at extremely small values of  $s'$  and  $E_{e^+e^-}$ .

If one would simply eliminate all events with secondary radiation of hadrons and leptons, one would arrive at a measurement of  $\Gamma(Z \rightarrow \tau^+\tau^-)$  significantly below (about 0.4%) the generally quoted inclusive value. Both real and virtual radiation are enhanced by the square of the large logarithm  $\ln(M_Z^2/m_{had}^2)$  times  $\ln(M_Z^2/m_l^2)$ . Because the coefficients of these logarithms only differ by sign, real and virtual corrections cancel to a large extent. This leads to a small contribution to the inclusive decay rate, as can be seen in the next section. Measurements of exclusive  $\tau$  pair production, however, are strongly affected. With this application in mind we proceed to the calculation of the virtual corrections.



$\sqrt{s}$	3.4552 GeV = $2 m_\tau$	4.2 GeV	10 GeV	$M_Z$
$F_{1,had}$	$7.45 \cdot 10^{-5}$	$3.55 \cdot 10^{-5}$	$2.69 \cdot 10^{-6}$	$-2.78 \cdot 10^{-4}$
$F_{2,had}$	$9.00 \cdot 10^{-6}$	$4.68 \cdot 10^{-6}$	$-3.21 \cdot 10^{-7}$	$-6.03 \cdot 10^{-8}$
$R_{\tau^+\tau^-had}^{virt}$	0	$5.89 \cdot 10^{-5}$	$4.45 \cdot 10^{-6}$	$-5.56 \cdot 10^{-4}$
$F_{1,e^+e^-}$	$1.50 \cdot 10^{-2}$	$5.84 \cdot 10^{-5}$	$-1.82 \cdot 10^{-4}$	$-8.94 \cdot 10^{-4}$
$F_{2,e^+e^-}$	$2.30 \cdot 10^{-3}$	$-4.26 \cdot 10^{-6}$	$-2.43 \cdot 10^{-6}$	$-8.21 \cdot 10^{-8}$
$R_{\tau^+\tau^-e^+e^-}^{virt}$	0	$7.78 \cdot 10^{-5}$	$-3.68 \cdot 10^{-4}$	$-1.79 \cdot 10^{-3}$
$F_{1,\mu^+\mu^-}$	$5.86 \cdot 10^{-5}$	$1.76 \cdot 10^{-5}$	$-5.98 \cdot 10^{-6}$	$-1.38 \cdot 10^{-4}$
$F_{2,\mu^+\mu^-}$	$7.74 \cdot 10^{-6}$	$1.74 \cdot 10^{-6}$	$-3.37 \cdot 10^{-7}$	$-2.57 \cdot 10^{-8}$
$R_{\tau^+\tau^-\mu^+\mu^-}^{virt}$	0	$2.82 \cdot 10^{-5}$	$-1.28 \cdot 10^{-5}$	$-2.77 \cdot 10^{-4}$
$F_{1,\tau^+\tau^-}$	$1.25 \cdot 10^{-6}$	$1.31 \cdot 10^{-6}$	$2.16 \cdot 10^{-6}$	$-1.08 \cdot 10^{-5}$
$F_{2,\tau^+\tau^-}$	$1.03 \cdot 10^{-7}$	$1.14 \cdot 10^{-7}$	$6.00 \cdot 10^{-8}$	$-3.73 \cdot 10^{-9}$
$R_{\tau^+\tau^-\tau^+\tau^-}^{virt}$	0	$2.08 \cdot 10^{-6}$	$4.47 \cdot 10^{-6}$	$-2.16 \cdot 10^{-5}$

Table 2: *Virtual corrections due to hadronic and leptonic vacuum polarisation for center of mass energies  $\sqrt{s} = 2m_\tau/4.2 \text{ GeV}/10 \text{ GeV}/M_Z$  for form factors and the resulting cross section as described in the text.*

### 3. Virtual radiation of hadrons

Virtual corrections to  $\tau$  pair production affect both Dirac and Pauli form factors,  $F_1$  and  $F_2$ . Leptonic corrections have been calculated in analytic form in [4] for the cases that the masses of the radiated leptons are much smaller than or equal to the  $\tau$  mass. The effect of virtual radiation of hadrons via hadronic vacuum polarisation of one exchanged photon, as depicted in Fig.1b, is given by an expression similar to eq. (1). For virtual radiation the phase space integration has to be extended to infinity corresponding to the dispersion integration of the absorptive part of the hadronic vacuum polarisation. The function  $F(s', s)$ , now representing the normalized cross section for the production of a  $\tau$  pair with an exchanged vector boson of mass  $\sqrt{s'}$ , may be easily calculated analytically and reads

$$F(s', s) = \left(\frac{\alpha}{\pi}\right)^2 \left[ \omega(3 - \omega^2) \left[ \text{Re}\widehat{F}_1(s', s) + \text{Re}\widehat{F}_2(s', s) \right] + \omega^3 \text{Re}\widehat{F}_2(s', s) \right], \quad (5)$$

where

$$\omega = \sqrt{1 - 4m_\tau^2/s}. \quad (6)$$

The functions  $\text{Re}\widehat{F}_{1,2}$  are given in [4] (eqs. (15) and (16)) and denote the real parts of the electromagnetic form factors arising from the exchange of a vector boson of mass  $\sqrt{s'}$ . The integral

$$R_{\tau^+\tau^-had}^{virt} = \frac{1}{3} \left(\frac{\alpha}{\pi}\right)^2 \int_{4m_\pi^2}^{\infty} \frac{ds'}{s'} R_{had}(s') F(s', s) \quad (7)$$

is calculated numerically. A similar formula applies to the form factors individually.

Virtual corrections from different hadronic intermediate states cannot be separated experimentally and contribute in a coherent manner. Their combined effect on the form factors and the rate are displayed in Table 2 for four characteristic energies. For completeness we also display the contributions from leptonic vacuum polarisation. Contributions from virtual electron pairs are obtained with analytical formulae derived in the limit  $m_e \ll m_\tau$  (see [4]). In the same reference an analytic

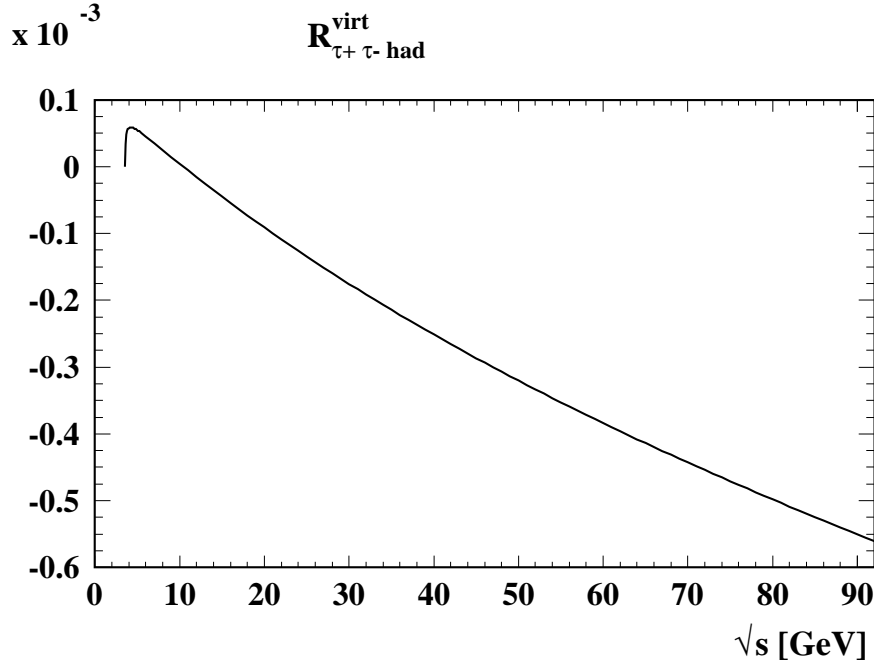


Figure 6: *Contribution to  $e^+e^- \rightarrow \tau^+\tau^-$  due to virtual radiation of hadrons.*

formula for virtual  $\tau$  pairs is also at hand. It is evident from Table 2 that these corrections must be taken into consideration in precision measurements of partial rates. Close to threshold the virtual corrections give a positive contribution to  $R$  as is illustrated in Fig. 6, where  $R_{\tau^+\tau^-}^{virt\ had}$  is plotted for the range  $2m_\tau < \sqrt{s} < M_Z$ . This is a consequence of the Coulomb attraction mediated by the exchange of a vector boson. Far above threshold the corrections are negative. They lead to a reduction of the exclusive decay rate of  $Z \rightarrow \tau^+\tau^-$  by nearly three per mill, exceeding the  $\mathcal{O}(\alpha)$  correction of  $3/4(\alpha/\pi) \approx 1.7 \cdot 10^{-3}$ . As mentioned above these negative corrections cancel for the most part the positive corrections from real emission, leaving a small positive overall correction. This remainder can to a large extent be absorbed into a running electromagnetic coupling constant  $\alpha(s)$  as discussed in [4].

#### 4. Corrections to $Z$ decays into $\mu^+\mu^-$ and $e^+e^-$

In [1, 2] analytical and numerical results were presented for real and virtual radiation of massive leptons or hadrons from the primary production of massless leptons. For completeness it seems appropriate to present in this paper a brief update of the hadronic radiation in  $Z$  decays to  $\mu^+\mu^-$  and  $e^+e^-$  together with a complete table for the radiation of leptons. Real and virtual radiation are presented in Tables 3 and 4 respectively. It is evident that exclusive determinations of  $Z \rightarrow e^+e^-$  or  $\mu^+\mu^-$  will become sensitive towards these corrections.

The results for  $R_{e^+e^-had}$  and  $R_{\mu^+\mu^-had}$  are  $\approx 6\%$  larger than our old value [2]. Half of this effect is due to the updated description of the continuum and 3% originate from the inclusion of the effective electromagnetic coupling constant  $\alpha$  (see also the appendix). Comparing our result for  $R_{e^+e^-}^{virt\ had}$  (taking  $\sqrt{s} = 93$  GeV) with the corresponding one in [1] the difference amounts to only 1%. Our results for the radiation of leptons are about 15% lower than those of [6], essentially a consequence of the different choice for  $\alpha$ . There the running electric coupling constant  $\alpha(M_Z^2)$  was chosen. However, radiation of leptons, in particular of electrons, is dominated by small  $s'$ . Therefore

secondary\primary	$e$	$\mu$	$\tau$
$e$	$2.78 \cdot 10^{-3}$	$2.53 \cdot 10^{-3}$	$1.82 \cdot 10^{-3}$
$\mu$	$3.32 \cdot 10^{-4}$	$3.31 \cdot 10^{-4}$	$2.94 \cdot 10^{-4}$
$\tau$	$3.23 \cdot 10^{-5}$	$3.21 \cdot 10^{-5}$	$3.13 \cdot 10^{-5}$
<i>hadrons</i>	$6.68 \cdot 10^{-4}$	$6.67 \cdot 10^{-4}$	$6.14 \cdot 10^{-4}$
Sum	$3.81 \cdot 10^{-3}$	$3.56 \cdot 10^{-3}$	$2.76 \cdot 10^{-3}$

Table 3: Real radiation  $R_{\text{primary,secondary}}$  for  $s = M_Z^2$ .

secondary\primary	$e$	$\mu$	$\tau$
$e$	$-2.75 \cdot 10^{-3}$	$-2.50 \cdot 10^{-3}$	$-1.79 \cdot 10^{-3}$
$\mu$	$-3.15 \cdot 10^{-4}$	$-3.14 \cdot 10^{-4}$	$-2.77 \cdot 10^{-4}$
$\tau$	$-2.24 \cdot 10^{-5}$	$-2.24 \cdot 10^{-5}$	$-2.16 \cdot 10^{-5}$
<i>hadrons</i>	$-6.09 \cdot 10^{-4}$	$-6.09 \cdot 10^{-4}$	$-5.56 \cdot 10^{-4}$
Sum	$-3.69 \cdot 10^{-3}$	$-3.44 \cdot 10^{-3}$	$-2.64 \cdot 10^{-3}$

Table 4: Virtual radiation  $R_{\text{primary,secondary}}^{\text{virt}}$  for  $s = M_Z^2$ .

the low energy scale adopted in this work is more appropriate.

Below we also list the high energy expansions (neglecting terms of order  $m_{1/2}^2/s$ ) of  $R_{f_1\bar{f}_1f_2\bar{f}_2}$  and  $R_{f_1\bar{f}_1f_2\bar{f}_2}^{\text{virt}}$  for the cases  $m_1 \gg m_2$ ,  $m_1 = m_2$  and  $m_1 \ll m_2$ , where  $m_1$  is the mass of the primary produced fermion  $f_1$  and  $m_2$  the mass of the secondary emitted fermion  $f_2$ . These formulae provide excellent approximations for  $\sqrt{s} = M_Z$  (better than one per mill in all cases except for  $f_2 = \tau$ , where the relative difference between complete and approximate result amounts to nearly 1%) and therefore can directly be applied to the corresponding leptonic  $Z$  partial widths.

$$\begin{aligned}
R_{f_1\bar{f}_1f_2\bar{f}_2}^{m_1 \gg m_2} &= \left(\frac{\alpha}{\pi}\right)^2 \left[ -\ln^2 \frac{m_2^2}{s} \frac{1}{6} \left( \ln \frac{m_1^2}{s} + 1 \right) \right. \\
&\quad + \ln \frac{m_2^2}{s} \left( \frac{1}{6} \ln^2 \frac{m_1^2}{s} - \frac{13}{18} \ln \frac{m_1^2}{s} + \frac{4}{3} \zeta(2) - \frac{53}{36} \right) \\
&\quad - \frac{1}{18} \ln^3 \frac{m_1^2}{s} + \frac{13}{36} \ln^2 \frac{m_1^2}{s} - \left( \frac{133}{108} + \frac{2}{3} \zeta(2) \right) \ln \frac{m_1^2}{s} \\
&\quad \left. + \frac{5}{3} \zeta(3) + \frac{32}{9} \zeta(2) - \frac{833}{216} - \frac{3}{4} \frac{m_2}{m_1} \pi^2 \right] \quad (8)
\end{aligned}$$

$$\begin{aligned}
R_{f_1\bar{f}_1f_2\bar{f}_2}^{m_1 = m_2} &= \left(\frac{\alpha}{\pi}\right)^2 \left[ -\frac{1}{18} \ln^3 \frac{m_2^2}{s} - \frac{19}{36} \ln^2 \frac{m_2^2}{s} + \frac{2}{3} \left( -\frac{73}{18} + \zeta(2) \right) \ln \frac{m_2^2}{s} \right. \\
&\quad \left. + \zeta(3) + \frac{11}{3} \zeta(2) - \frac{1829}{216} \right] \quad (9)
\end{aligned}$$

$$\begin{aligned}
R_{f_1\bar{f}_1f_2\bar{f}_2}^{m_1 \ll m_2} &= \left(\frac{\alpha}{\pi}\right)^2 \left[ -\frac{1}{18} \ln^3 \frac{m_2^2}{s} - \frac{19}{36} \ln^2 \frac{m_2^2}{s} + \frac{2}{3} \left( -\frac{73}{18} + \zeta(2) \right) \ln \frac{m_2^2}{s} \right. \\
&\quad \left. + \frac{5}{3} \zeta(3) + \frac{19}{9} \zeta(2) - \frac{2123}{324} \right] \quad (10)
\end{aligned}$$

$$\begin{aligned}
R_{f_1\bar{f}_1f_2\bar{f}_2}^{m_1 \gg m_2, virt} &= \left(\frac{\alpha}{\pi}\right)^2 \left[ \ln^2 \frac{m_2^2}{s} \frac{1}{6} \left( \ln \frac{m_1^2}{s} + 1 \right) \right. \\
&\quad + \ln \frac{m_2^2}{s} \left( -\frac{1}{6} \ln^2 \frac{m_1^2}{s} + \frac{13}{18} \ln \frac{m_1^2}{s} - \frac{4}{3} \zeta(2) + \frac{11}{9} \right) \\
&\quad + \frac{1}{18} \ln^3 \frac{m_1^2}{s} - \frac{13}{36} \ln^2 \frac{m_1^2}{s} + \left( \frac{133}{108} + \frac{2}{3} \zeta(2) \right) \ln \frac{m_1^2}{s} \\
&\quad \left. - \frac{2}{3} \zeta(3) - \frac{32}{9} \zeta(2) + \frac{67}{27} + \frac{3}{4} \frac{m_2}{m_1} \pi^2 \right] \quad (11)
\end{aligned}$$

$$R_{f_1\bar{f}_1f_2\bar{f}_2}^{m_1 = m_2, virt} = \left(\frac{\alpha}{\pi}\right)^2 \left[ \frac{1}{18} \ln^3 \frac{m_2^2}{s} + \frac{19}{36} \ln^2 \frac{m_2^2}{s} + \frac{2}{3} \left( \frac{265}{72} - \zeta(2) \right) \ln \frac{m_2^2}{s} - \frac{11}{3} \zeta(2) + \frac{383}{54} \right] \quad (12)$$

$$\begin{aligned}
R_{f_1\bar{f}_1f_2\bar{f}_2}^{m_1 \ll m_2, virt} &= \left(\frac{\alpha}{\pi}\right)^2 \left[ \frac{1}{18} \ln^3 \frac{m_2^2}{s} + \frac{19}{36} \ln^2 \frac{m_2^2}{s} + \frac{2}{3} \left( \frac{265}{72} - \zeta(2) \right) \ln \frac{m_2^2}{s} \right. \\
&\quad \left. - \frac{2}{3} \zeta(3) - \frac{19}{9} \zeta(2) + \frac{3355}{648} \right] \quad (13)
\end{aligned}$$

Results for virtual corrections were first obtained in [4], [10] and [1] for the cases  $m_1 \gg m_2$ ,  $m_1 = m_2$  and  $m_1 \ll m_2$ , respectively. Those for real radiation are taken from [4] for  $m_1 \gg m_2$  and from [2, 3] for  $m_1 \ll m_2$ . The formula for real radiation with  $m_1 = m_2$  is new. The leading cubic logarithms for all these cases can also be found in [11]. Note that in (8) and (11) linear mass corrections  $\sim m_2/m_1$  are included. They significantly improve the quality of the approximations, especially in the case  $m_1 = m_\tau$ ,  $m_2 = m_\mu$ . Neglecting these linear mass corrections the value of say  $R_{\tau^+\tau^-\mu^+\mu^-}^{m_1 \gg m_2, virt}$  for the energy  $\sqrt{s} = 20$  GeV differs from the value based on numerical integration by 4%, while including them leads to a difference of only three per mill. Of course, for higher energies the latter difference decreases and amounts to eight per mill vs. half a per mill for  $\sqrt{s} = M_Z$ . There are no linear mass corrections to the other high energy approximations. It is an interesting fact that the complete results for these linear mass corrections, valid for all energies above threshold, are remarkably simple:

$$R_{f_1\bar{f}_1f_2\bar{f}_2, linear}^{m_1 \gg m_2} = -\frac{3}{8} \omega (3 - \omega^2) \frac{m_2}{m_1} \pi^2, \quad (14)$$

$$R_{f_1\bar{f}_1f_2\bar{f}_2, linear}^{m_1 \gg m_2, virt} = \frac{3}{8} \frac{1 + \omega^2}{\omega} \frac{m_2}{m_1} \pi^2 \quad (15)$$

with  $\omega$  defined as in (6). They are in very close relation to the non-analytic linear vector boson mass terms of the corresponding one loop results denoted by  $F$ , eqs. (1) and (5). The difference between (14) and (15) can be reproduced by the analogous linear mass correction in the two loop relation between pole and running masses, see [12].

Again, concerning the total  $Z$  decay rate, it is obvious from eq. (8)–(13) that by adding the corresponding real and virtual contributions the dominant logarithmic terms cancel, leaving the result

$$R_{f_1\bar{f}_1f_2\bar{f}_2} + R_{f_1\bar{f}_1f_2\bar{f}_2}^{virt} = \left(\frac{\alpha}{\pi}\right)^2 \left[ \frac{1}{4} \ln \frac{s}{m_2^2} + \zeta(3) - \frac{11}{8} \right] \quad (16)$$

which is universal for all three mass constellations in the high energy limit. As mentioned in the previous section the remaining logarithm can be absorbed into the running coupling constant  $\alpha(s)$ , leaving a tiny term  $\sim (\alpha/\pi)^2$  without logarithm.

For completeness we also present the prediction for the radiation of hadrons from primary electrons and muons. In this case the result can be expressed in terms of the moments

$$R_n = \int_0^1 \frac{dx \ln^n x}{x n!} \left( R_{had}(4m^2/x) - R_{had}(\infty) \right) \quad (17)$$

leading to the following formulae for real [2] and for virtual [1] radiation ( $l = e, \mu$ )

$$R_{l+l-had} =$$

$$\frac{1}{6} \left( \frac{\alpha}{\pi} \right)^2 \left\{ R_{had}(\infty) \left[ \frac{1}{3} \ln^3 \frac{s}{4m_\pi^2} - \frac{3}{2} \ln^2 \frac{s}{4m_\pi^2} + (-2\zeta(2) + 5) \ln \frac{s}{4m_\pi^2} + \left( 6\zeta(3) + 3\zeta(2) - \frac{19}{2} \right) \right] \right. \\ \left. + R_0 \left[ \ln^2 \frac{s}{4m_\pi^2} - 3 \ln \frac{s}{4m_\pi^2} - 2\zeta(2) + 5 \right] + R_1 \left[ 2 \ln \frac{s}{4m_\pi^2} - 3 \right] + 2R_2 \right\}, \quad (18)$$

$$R_{l+l-had}^{virt} =$$

$$\frac{1}{6} \left( \frac{\alpha}{\pi} \right)^2 \left\{ R_{had}(\infty) \left[ -\frac{1}{3} \ln^3 \frac{s}{4m_\pi^2} + \frac{3}{2} \ln^2 \frac{s}{4m_\pi^2} + \left( 2\zeta(2) - \frac{7}{2} \right) \ln \frac{s}{4m_\pi^2} - 3\zeta(2) + \frac{15}{4} \right] \right. \\ \left. + R_0 \left[ -\ln^2 \frac{s}{4m_\pi^2} + 3 \ln \frac{s}{4m_\pi^2} + 2\zeta(2) - \frac{7}{2} \right] + R_1 \left[ -2 \ln \frac{s}{4m_\pi^2} + 3 \right] - 2R_2 \right\}. \quad (19)$$

The evaluation of (17) gives

$$\begin{aligned} R_{had}(\infty) &= 4.31, \\ R_0 &= -11.15, \\ R_1 &= 25.05, \\ R_2 &= -48.00 \end{aligned} \quad (20)$$

where we used the dressed  $R_{had}(s')$  including the narrow resonances and  $\sqrt{s'} = 100$  GeV as the integration cutoff. The values of the moments individually depend on the choice of this cutoff (and correspondingly  $R_{had}(\infty)$ ), but we have checked that the results of (18) and (19) are identical for all cutoff energies above 40 GeV. For the derivation of eqs. (18) and (19) the approximation  $m_l \ll m_\pi$  was essential. The relative difference between the asymptotic formulae and the complete numerical results is at most 0.2% for  $\sqrt{s} = M_Z$ . For lower energies, of course, the difference increases. Similar formulae for radiation off the primary tau pair provide a poor approximation to the true answer for real and virtual radiation individually, but are adequate for the sum, which is identical to the electron and muon case (see also Tables 3 and 4). For the sum of real and virtual radiation of leptons and hadrons at  $\sqrt{s} = M_Z$ , which is valid for all three lepton channels  $f_1 = e, \mu, \tau$ , one arrives at

$$\begin{aligned} &R_{f_1 \bar{f}_1 had} + R_{f_1 \bar{f}_1 had}^{virt} + \sum_{f_2=e,\mu,\tau} \left( R_{f_1 \bar{f}_1 f_2 \bar{f}_2} + R_{f_1 \bar{f}_1 f_2 \bar{f}_2}^{virt} \right) \\ &= \frac{3}{4} \left[ \frac{\alpha(M_Z^2)}{\pi} - \frac{\alpha}{\pi} \right] + \left( \frac{\alpha}{\pi} \right)^2 \left[ \zeta(3) - \frac{23}{24} \right] \left( R_{had}(\infty) + \sum_{f_2=e,\mu,\tau} Q_{f_2}^2 \right) \\ &\approx 0.12 \cdot 10^{-3}, \end{aligned} \quad (21)$$

where the usual definition of the running electromagnetic coupling constant

$$\frac{1}{\alpha(s)} - \frac{1}{\alpha} = \Pi(s) \quad (22)$$

was employed. Here the hadronic contributions to the photon vacuum polarisation have also been parametrized by the moments defined in (17):

$$\Pi(s) \xrightarrow{s \rightarrow \infty} -\frac{1}{3\pi} \left[ \sum_{i=e,\mu,\tau} \left( \ln \frac{s}{m_i^2} - \frac{5}{3} \right) + R_{had}(\infty) \ln \frac{s}{4m_\pi^2} + R_0 \right]. \quad (23)$$

The differential distribution  $dR_{l+l-had}/ds'_{had}$  for the case of massless leptons is given in closed form (see eqs. (1) and (2) of [2]),  $dR_{l+l-had}/dE_{had}$ , of course, has to be calculated numerically. The predicted distributions for the radiation of hadrons and of  $e^+e^-$  pairs off primary produced muon

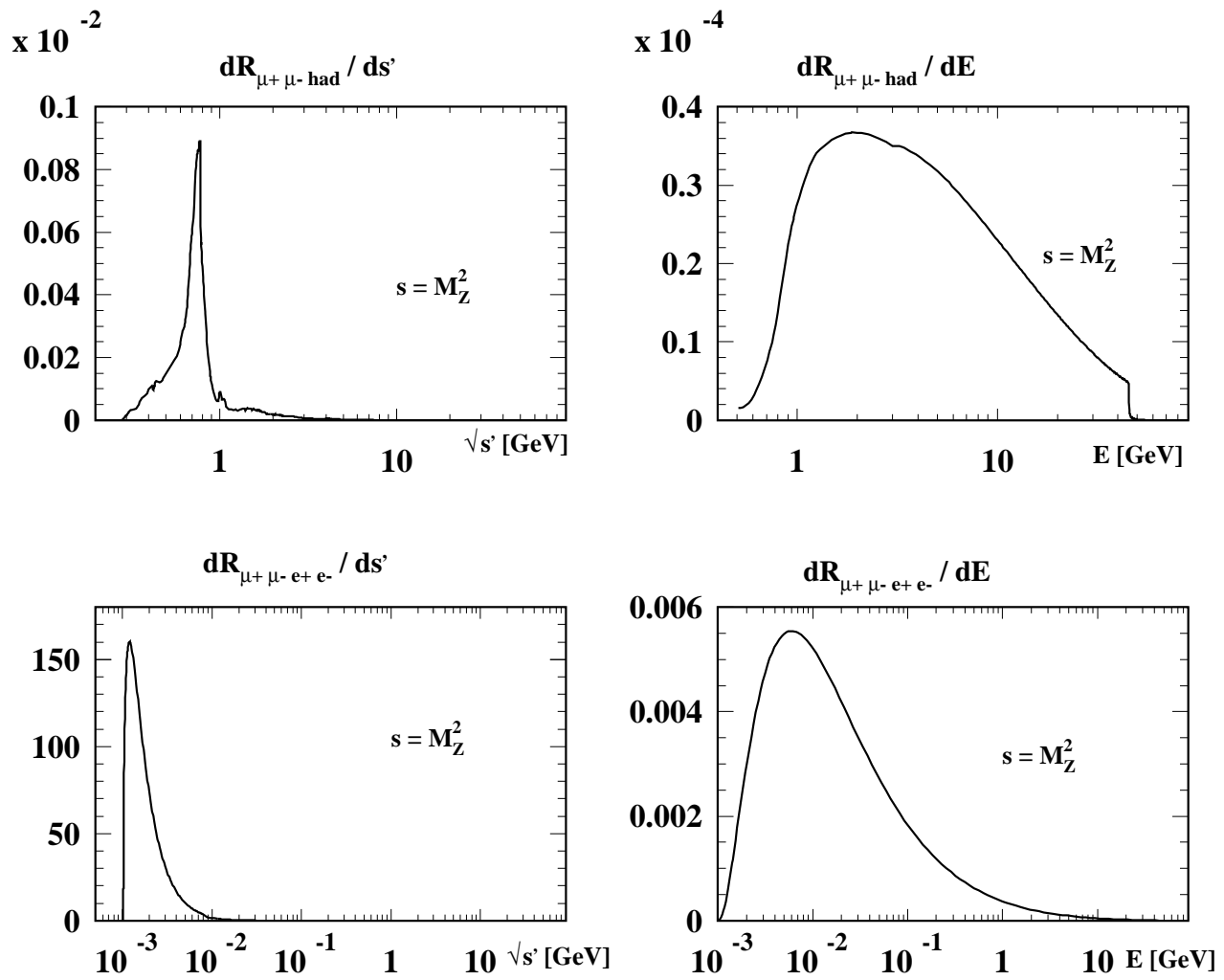


Figure 7: Differential distributions for real emission of hadrons and of  $e^+e^-$  pairs in  $\mu$  pair production for  $\sqrt{s} = M_Z$ .

pairs are shown<sup>4</sup> in Fig. 7. Again the dominant configuration consists of an  $\mu^+\mu^-$  with invariant mass fairly close to  $M_Z$  and a soft hadronic or  $e^+e^-$  system.

## 5. Summary

A comprehensive treatment of the radiation of hadronic final states from a primary  $\tau$  pair is presented, which is applicable over the full energy range of interest in the foreseeable future. In the low energy region real as well as virtual radiation is small, typically at the level of  $10^{-4}$  compared to the primary reaction. The situation is entirely different for a c.m. energy around 90 GeV. In this case important differences arise between “inclusive” and “exclusive” measurements of the  $Z \rightarrow \tau^+\tau^-$  rate, in particular if radiation of the various hadronic and fermionic channels is collected, or eliminated by experimental cuts. We have presented differential distributions with respect to the invariant mass and the energy of the hadronic system, and for comparison the same quantities for the radiation of electron–positron pairs. It is evident that all distributions are peaked at small masses and energies respectively. The calculation of the rate for hadronic radiation must necessarily rely on a numerical integration of experimental data. Leptonic radiation, on the other hand, can be calculated analytically for the mass assignments of interest. Handy formulae are presented for different mass assignments which are applicable in the high energy limit, and which are valid up to terms of order  $m_{lept}^2/s$ . They may be useful also for other applications.

*Acknowledgment:* We would like to thank F. Jegerlehner and S. Eidelman for providing their compilation of data and discussing its proper treatment. We are also grateful to K. Chetyrkin, W. Hollik and D. Schaile for helpful discussions. One of the authors (J.H.K.) would like to thank the SLAC theory group for hospitality, and the Volkswagen–Stiftung grant I/70 453 for generous support.

## Appendix: $R_{had}(s')$

In our calculation we used experimental data for  $R_{had}(s')$  as presented in a recent publication by F. Jegerlehner and S. Eidelman[7]. For a detailed discussion we refer the reader to this work.

In the region close to the  $\pi^+\pi^-$  threshold where no experimental data are available we use the chiral expansion of the pion form factor (eq. (18) of [7]). The continuum– and  $\rho$ –contributions are parametrized by weighted averages of experimental data from various experiments. From 318 MeV up to 810 MeV these are given in terms of the pion form factor  $|F_\pi|^2$ . The continuum from 810 MeV up to 40 GeV (above which we use the prediction of perturbation theory) is well described by weighted averages of  $R_{had}(s)$ . At this point two comments are in order: The higher resonances  $\psi(4040)$ ,  $\psi(4160)$  and  $\psi(4415)$  are included in the weighted averages of the continuum data (as can be seen in Fig. 7 of [7]) whereas the resonances  $\omega$ ,  $\Phi$ ,  $J/\psi(1S)$ ,  $\psi(2S)$ ,  $\psi(3770)$  and the  $\Upsilon$ –family (six resonances) are treated in the narrow width approximation as described above.

All experimental values of  $R_{had}$  (and  $|F_\pi|^2$ ) are given as “undressed” ( $\equiv$  lowest order in QED) quantities. In order to resum all additional self–energy insertions in the photon propagator we use for

---

<sup>4</sup>The figure for  $dR_{l+l-had}/ds'_{had}$  does not include the narrow resonances. The missing contributions to  $R_{l+l-had}$  are  $\omega$ :  $2.33 \cdot 10^{-5}$ ,  $\phi$ :  $3.56 \cdot 10^{-5}$ ,  $J/\psi$ :  $2.95 \cdot 10^{-5}$  and  $\Upsilon$ :  $8.33 \cdot 10^{-7}$ .

the integration of (1), (2) and (7) the “dressed” quantity

$$R_{had}^{dressed}(s) = \left( \frac{\alpha(s)}{\alpha} \right)^2 R_{had}(s), \quad \alpha(s) = \frac{\alpha}{1 - \Delta\alpha}. \quad (24)$$

In the low energy region up to  $\sqrt{s'} = 3$  GeV most experiments only used the leptonic contribution of  $\Delta\alpha$  to extract one-particle-irreducible quantities from the measured cross-sections. For that reason we take  $\Delta\alpha = \Delta\alpha_{lep}$  in this region. For all other energies

$$\Delta\alpha = \Delta\alpha_{lep} + \Delta\alpha_{had}.$$

As mentioned above these corrections led to an increase of the result by a factor of  $\approx 1.03$ . We also calculated the effect of  $\Delta\alpha_{lep}(s)$  on our results, comparing the full one loop expression of the fermionic part of the photon self energy with the leading logarithmic behaviour (as it appears in the renormalization group “running  $\alpha$ ”). The difference of  $\approx 0.5\%$  may be considered as a crude estimate of other effects not taken into account via the implicit resummation by using  $\alpha(s)$  and is smaller than the claimed accuracy of our calculation.

## References

1. B.A. Kniehl, M. Krawczyk, J.H. Kühn and R.G. Stuart, *Phys. Lett.* **B 209** (1988) 337.
2. A.H. Hoang, M. Jezabek, J.H. Kühn and T. Teubner, *Phys. Lett.* **B 325** (1994) 495 and *Phys. Lett.* **B 327** (1994) 439 (Erratum).
3. A.H. Hoang, M. Jezabek, J.H. Kühn and T. Teubner, *Phys. Lett.* **B 338** (1994) 330.
4. A.H. Hoang, J.H. Kühn and T. Teubner, Univ. of Karlsruhe preprint TTP95-10, to be published in *Nucl. Phys.* **B**.
5. S. Jadach, M. Skrzypek and M. Martinez, *Phys. Lett.* **B 280** (1992) 129.
6. E.W.N. Glover, R. Kleiss, J.J. van der Bij, *Z. Phys.* **C 47** (1990) 435 and refs. therein.
7. S. Eidelman and F. Jegerlehner, PSI-PR-95-1, BudkerINP 95-5 and hep-ph9502298.
8. B.A. Kniehl and J.H. Kühn, *Nucl. Phys.* **B 329** (1990) 547.
9. *Review of Particle Properties*, *Phys. Rev.* **D 50** (1994) 1173.
10. G.J.H. Burgers, *Phys. Lett.* **B 164** (1985) 167.
11. V.N. Baier, V.S. Fadin and V.A. Khoze, *Soviet Physics JETP Lett.* **23** (1966) 104.
12. N. Gray, D.J. Broadhurst, W. Grafe and K. Schilcher, *Z. Phys.* **C 48** (1990) 673.